
Fatigue-crack growth properties of thin-walled superelastic austenitic Nitinol tube for endovascular stents

J.M. Stankiewicz, S.W. Robertson, R.O. Ritchie

Department of Materials Science and Engineering, University of California, Berkeley, California 94720

Received 28 July 2006; revised 31 August 2006; accepted 15 September 2006

Published online 22 December 2006 in Wiley InterScience (www.interscience.wiley.com). DOI: 10.1002/jbm.a.31100

Abstract: Over the past 10 years, the superelastic nickel–titanium alloy Nitinol has found widespread application in the manufacture of small-scale biomedical devices, such as self-expanding endovascular stents. Although conventional stress/strain-life (S/N) analyses are invariably used as the primary method for design against fatigue loading and for predicting safe lifetimes, fracture mechanics-based methodologies provide a vital means of assessing the quantitative effect of defects on such lifetimes. Unfortunately, fracture mechanics studies on fatigue in Nitinol are scarce, and most results do not pertain to the (thin-walled tube) product forms that are typically used in the manufacture of endovascular stents. In the current work, we document the basic fatigue-crack growth properties of flattened thin-walled ($\sim 400\ \mu\text{m}$ thick) Nitinol tubing in a 37°C air environment. Crack-growth behavior is characterized over a

wide range of growth rates (~ 6 orders of magnitude) and load ratios, that is, as a function of the alternating and maximum stress intensities, at 50 Hz. Limited experiments at both 5 and 50 Hz were also performed in 37°C air and simulated body fluid to determine whether the cyclic frequency affects the fatigue behavior. Fatigue-crack growth-rate properties in such thin-walled Nitinol tube are found to be quite distinct from limited published data on other (mainly bulk) product forms of Nitinol, for example, bar and strip, both in terms of the relative fatigue thresholds and the variation in steady-state growth rates. © 2006 Wiley Periodicals, Inc. *J Biomed Mater Res* 81A: 685–691, 2007

Key words: Nitinol; stents; fatigue; crack growth; frequency effects; load ratio effects

INTRODUCTION

Nitinol is an approximately equiatomic alloy of nickel and titanium that exhibits superelastic and shape-memory properties. These unique mechanical properties make it a premier choice for the manufacture of biomedical implants, such as self-expanding endovascular stents. They result from the occurrence of a phase transformation, from a cubic austenitic parent phase to a monoclinic martensitic daughter phase, on the application of stress or due to a decrease in temperature.¹ For most stent applications, Nitinol is thermomechanically treated to have an austenite finish temperature, A_f , of typically 28°C , that is slightly below the human body temperature, such that the implanted alloy is in the superelastic

austenite condition. Of note here is that on transformation to martensite, there is a small negative dilation (reported to be $\sim 0.39\text{--}0.54\%^{2,3}$), which may locally increase the tensile stresses developed ahead of a crack,⁴ thereby degrading the fracture toughness and fatigue-crack growth properties. This is opposite to the effect seen in transformation-toughened ceramics, where an increase in volume with transformation creates a zone of compressive stress surrounding a crack, thereby increasing the extrinsic resistance to fracture and fatigue.^{5,6}

With respect to fatigue, stents are subjected to cyclic stresses *in vivo* from the expansion and contraction of the blood vessels, which can lead to fatigue damage and curtail their useful life. For example, measurements of strains experienced in these vessels of the body show a 3–10% change in diameter with a pulse pressure of 100 mmHg,⁷ with exact values dependent upon many variables such as vessel compliance or patient blood pressure. Nitinol stents are typically designed for a minimum lifetime of 10 years after implantation⁸; since physiological loading typically amounts to roughly 40 million cycles per year, this means that they must survive more

Correspondence to: R.O. Ritchie; e-mail: RORitchie@lbl.gov

Contract grant sponsor: National Science Foundation; contract grant number: CMS-0409294

Contract grant sponsor: Nitinol Devices and Components, Inc., Fremont, CA

than 4×10^8 cycles of fatigue loading in service. Although conventional stress/strain-life (S/N) analyses are invariably used as the primary method of fatigue design and life prediction,^{9–14} fracture mechanics-based methodologies provide the best means of assessing the quantitative effect of defects, and are particularly important for determining required detectable flaw sizes and conservatively estimating fatigue lifetimes in the presence of such flaws. Unfortunately, quantitative information on fatigue-crack propagation behavior in Nitinol, characterized using fracture mechanics, is rarely found in the literature; moreover, published results^{3,15–17} are primarily on bulk Nitinol material and do not pertain to the thin-walled ($\sim 400\text{-}\mu\text{m}$ thick) tubing that is typically used in the manufacture of endovascular stents. Both the well-documented traditional S/N (based on crack initiation and/or total life) and fracture mechanics-based methodologies are important in the design of biomedical devices and complement, rather than compete, with one another. Specifically, the total-life approach may be used to estimate safe *in vivo* operating stresses/strains and accounts for both crack initiation and propagation, whereas the fracture mechanics approach employed here includes only the crack-growth phase of fatigue, and is specifically designed for the determination of critical flaw sizes that may cause premature failure of the device.

As the transformation and volumetric changes in Nitinol are highly dependent on its microstructure and processing, which in turn have a marked influence on mechanical properties (e.g., Ref. 18), a prime objective of the current research is to characterize the basic fatigue-crack growth properties of superelastic austenitic Nitinol on material (flattened thin-walled tube), heat-treated and processed in similar fashion to that used in the manufacture of endovascular stents. Results are compared to the limited fatigue-crack growth data that have been published on bulk bar^{3,15,16} and thin strip¹⁷ material. Specifically, the effects of positive load ratio* (ratio of minimum to maximum stress or stress intensity) and cyclic frequency are examined at 5 and 50 Hz. The effect of frequency is deemed to be of particular importance, as virtually all fatigue evaluations on biomedical Nitinol to date have been conducted (for expediency) at frequencies far in excess of those relevant to physiological loading.

EXPERIMENTAL PROCEDURES

Nitinol material, identical to that used for endovascular stents, was provided by Nitinol Devices and Components

*Also referred to as the force ratio.

(Fremont, CA), with a composition of 50.8 at % Ni (balance Ti). Samples for fatigue-crack growth testing were in the form of 0.41-mm thick compact-tension, C(T), specimens (with a 9.9 mm width and a 1.93 mm starter notch), which were laser-cut from unrolled, flattened and shape-set thin-walled tubes, similar to that used in the manufacture of stents. Subsequent thermal processing (“tuning”) resulted in a material with an A_f of $\sim 28^\circ\text{C}$ (as determined by differential scanning calorimetry); this material was thus capable of forming stress-induced martensite during fatigue experiments at 37°C . Following the flattening, cutting, and tuning procedures, the specimens were electropolished to produce a stent-like finish by eliminating the irregular thermal oxide layer from the drawing process and forming an amorphous passive Ti_xO_y layer. Although this fabrication process invariably leaves some residual stresses in the specimens, they are produced in such a way as to mimic the microstructure, surface, and internal stresses of a finished endovascular stent, such that the fatigue-crack growth properties in such a device can be appropriately estimated.

The orientation of the prenotch, and hence the crack-propagation direction, was 45° to the tube drawing direction; this crack direction represents the path of least tensile strain required for the phase transformation, as determined by texture experiments.¹⁸ Interestingly, alternative orientations, specifically with the prenotch oriented parallel to the circumference of the tube, resulted in crack paths which diverged at 45° from the expected mode I (maximum tensile stress) direction.

Fatigue-crack propagation tests were carried out on an electro servo-hydraulic mechanical test system (MTS model 831, MTS Systems, Eden Prairie, MN), in general accordance with ASTM Standard E 647.¹⁹ In order to study the role of alternating versus maximum stresses, tests were performed under force control at a range of positive load ratios ($R = K_{\min}/K_{\max}$), specifically at $R = 0.1, 0.5,$ and 0.7 , in a controlled environment of $(37 \pm 0.1)^\circ\text{C}$ air. While the majority of the testing was conducted at 50 Hz (sine wave), crack-growth experiments were also performed at 5 Hz at 37°C in both air and simulated body fluid to determine the effect, if any, of test frequency on crack-growth rates. The simulated body fluid comprised Hanks’ balanced saline solution (HBSS) at a pH of 7.4; deleterious bacterial growth was inhibited by Gentamicin at a ratio of 2 mL/L of HBSS.

Crack lengths were continuously monitored *in situ*, with a resolution of 0.01 mm, using load-point compliance-based methodology; crack length values were periodically verified during fatigue testing, using optical microscopy, with the compliance and visual measurements agreeing to within $\pm 5\%$. Stress-intensity K solutions were determined from handbook solutions.¹⁹ Fatigue threshold ΔK_{th} values, operationally defined as the stress-intensity range, $\Delta K = K_{\max} - K_{\min}$, to give a growth rate of 10^{-10} m/cycle (based on linear extrapolation of data between 10^{-9} and 10^{-10} m/cycle),¹⁹ were approached using computer-controlled continuous force shedding at a K -gradient of $-0.20/\text{mm}$. Fatigue-crack growth rates (da/dN) are presented both as a function of stress-intensity range, $\Delta K = K_{\max} - K_{\min}$, and the maximum stress intensity, K_{\max} .

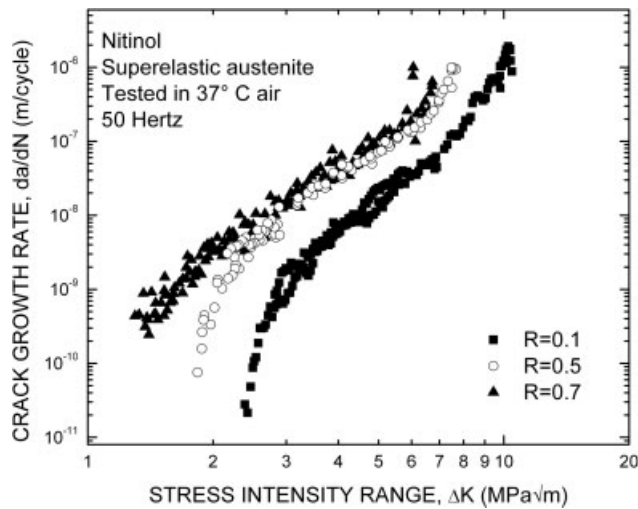


Figure 1. Variation in fatigue-crack propagation rates as a function of the stress-intensity range, ΔK , for Nitinol in the superelastic austenite condition at load ratios of $R = 0.1, 0.5$, and 0.7 , showing how the fatigue thresholds are decreased and near-threshold growth rates are increased at higher R . Tests were performed in 37°C air at a frequency of 50 Hz using $\sim 400\text{-}\mu\text{m}$ thick C(T) specimens laser-cut from flattened thin-walled Nitinol tubing.

RESULTS AND DISCUSSION

Effect of load ratio

The variation in fatigue-crack propagation rates, as a function of the stress-intensity range, ΔK , is shown for Nitinol thin-walled superelastic austenitic tubing in Figure 1 for load ratios of $R = 0.1, 0.5$, and 0.7 . Data span five decades of growth rates from $\sim 10^{-11}$ to 10^{-6} m/cycle, and show Paris power-law behavior between $\sim 10^{-9}$ and 10^{-7} m/cycle, namely

$$da/dN = C(\Delta K)^m \tag{1}$$

where C and m are scaling constants. Similar to most metallic materials,^{20,21} these results clearly show how growth rates are increased with increasing ΔK , and how raising the load ratio further accelerates near-threshold growth rates and decreases the ΔK_{th} fatigue thresholds. Specifically, ΔK_{th} thresholds are reduced from $2.5\text{ MPa}\sqrt{\text{m}}$ at $R = 0.1$ – $1.4\text{ MPa}\sqrt{\text{m}}$ at $R = 0.7$. As noted previously,¹⁵ these threshold values for Nitinol are characteristically very low compared to most other metallic and intermetallic materials.^{20,21}

Although beyond the scope of the present work, the significant effect of the load ratio on the fatigue thresholds can generally be ascribed to crack closure phenomena (e.g., Refs. 20–22), primarily associated with the crack wedging action of surface oxide debris²³ and/or fracture surface asperities.^{24–26} In the present case, as cyclic crack-tip opening displacements,

estimated²⁷ close to the threshold, are small ($\Delta\text{CTOD} \sim 20\text{--}50\text{ nm}$) compared to the scale of fracture surface roughness ($\sim 5\text{ }\mu\text{m}$), it is probable that the roughness-induced closure mechanism is most responsible for the load ratio effect. This is consistent with the fact that the load ratio dependence on growth rates is progressively diminished with increasing ΔK levels, where the crack-tip opening displacements become much larger.

In Figure 2, the growth-rate data from Figure 1 are plotted as a function of the maximum stress intensity. Comparison of Figures 1 and 2 clearly indicates that growth rates in Nitinol are a function of both ΔK and K_{max} and as such, a simple Paris power-law descriptions [(e.g., Eq. (1)), become inadequate. An alternative approach is to use a modified Paris law, which quantifies the effect of both ΔK and K_{max} on crack-growth rates,²¹ namely

$$da/dN = C'(K_{max})^n(\Delta K)^p \tag{2}$$

where $C' = C(1 - R)^m$ and $m = n + p$. Measured exponents, based on least-square curve fits to the data in Figures 1–2, are listed in Table I, where it is apparent that the ΔK dependence is some 2–3 times larger than that due to K_{max} . Such results are consistent with most reported data for ductile metallic materials (where $p > n$)²¹ and intermetallic alloys (where $p \sim n$),^{21,28,29} and in sharp contrast to brittle ceramics (where $p \ll n$).^{21,30}

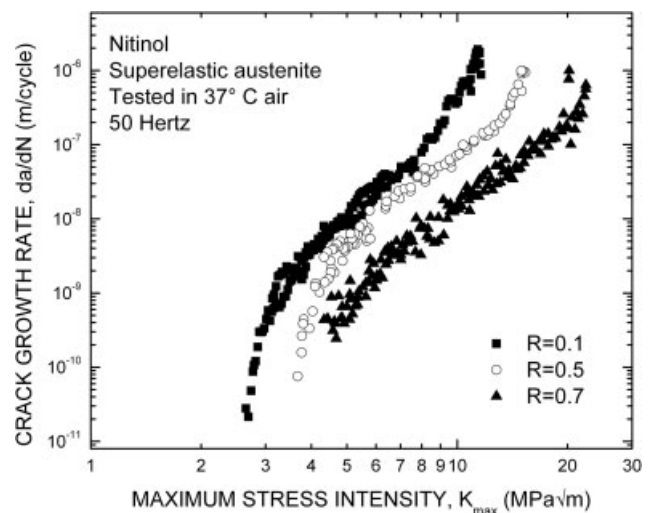


Figure 2. Variation in fatigue-crack propagation rates as a function of the maximum stress intensity, K_{max} , for Nitinol in the superelastic austenite condition at load ratios of $R = 0.1, 0.5$, and 0.7 , based on tests performed in 37°C air at a frequency of 50 Hz , using $\sim 400\text{-}\mu\text{m}$ thick C(T) specimens laser-cut from flattened thin-walled Nitinol tubing. By comparison to Figure 1, it is apparent that growth rates are a function of both ΔK and K_{max} .

TABLE I
Scaling Constants in the Paris Law [Eq. (1)] and Modified Paris Law [Eq. (2)] for Nitinol Thin-Walled Tube Samples

Load Ratio, R	m	C (m/cycle/(MPa \sqrt{m}) ^{m})	n	p	C' (m/cycle/(MPa \sqrt{m}) ^{m})
0.1	4.21	1.88×10^{-11}	1.53	2.68	1.60×10^{-11}
0.5	3.43	2.96×10^{-10}	0.75	2.68	1.76×10^{-10}
0.7	3.71	2.49×10^{-10}	1.03	2.68	7.21×10^{-11}

Effect of cyclic frequency

As noted earlier, most fatigue testing of Nitinol materials and components for biomedical applications is performed at relatively high frequencies, typically at 30–60 Hz; this is of course significantly greater than the physiological loading conditions, for example, a natural heartbeat, which is closer to 1 Hz. What is somewhat unsettling about this is that crack-growth rates per cycle (at fixed ΔK , K_{\max}) can often be accelerated at lower frequencies, because there is more time during the fatigue cycle, for example, for corrosion processes to occur (e.g., Ref. 31).^{*} The implications of this are that life predictions may not be conservative when based on such higher frequency data. Despite this, few studies to date have examined the influence of frequency on crack-growth behavior in Nitinol.

Since it is difficult owing to time constraints to determine the entire growth-rate relationship at low frequencies, experiments in the current study were performed at constant ΔK in both 37°C air (at $R = 0.1$) and HBSS environments (at $R = 0.5$); see Figure 3. Specifically, a crack was allowed to propagate for several millimeters at 50 Hz under steady-state conditions at a constant ΔK , for constant ΔK levels of 3.8 and 5.4 MPa \sqrt{m} in air, and 3 and 5 MPa \sqrt{m} in HBSS; the frequency was then lowered to 5 Hz (with all other conditions held constant), and the change in growth rate was monitored as the crack grew a further few millimeters. For experiments in air [Fig. 3(a)], the fatigue-crack growth rate, da/dN , at $\Delta K = 3.8$ MPa \sqrt{m} was slightly slower during the 5 Hz (6×10^{-9} m/cycle) versus the 50 Hz test (7×10^{-9} m/cycle), representing a 14% decrease in growth rate. Growth rates in air at 5.4 MPa \sqrt{m} were identical at the two testing frequencies (2×10^{-8} m/cycle). For corresponding experiments in HBSS, the growth rate at $\Delta K = 5$ MPa \sqrt{m} was virtually identical at

^{*}There may also be an inherent effect of strain rate associated with the effect of frequency on fatigue properties. In fatigue, however, these effects generally require several orders of magnitude change in frequency to be seen. Moreover, studies on strain-rate effects in Nitinol show that stress-induced martensite is relatively strain-rate insensitive for rates up to as high as 10^3 /s.^{32–34}

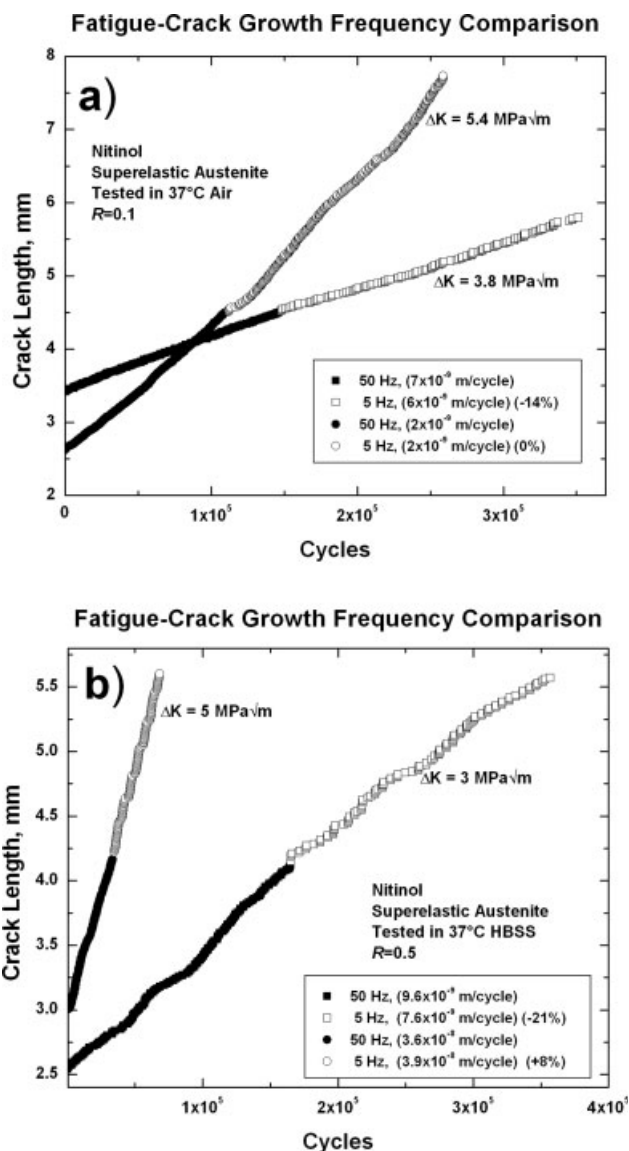


Figure 3. Constant ΔK experiments show effect of cyclic frequency on crack-growth rates in superelastic austenitic Nitinol at 37°C in environments of (a) air with $R = 0.1$, $\Delta K = 3.8$ and 5.4 MPa \sqrt{m} and (b) HBSS with $R = 0.5$, $\Delta K = 3$ and 5 MPa \sqrt{m} . These experiments, at constant ΔK values within the steady-state (Paris) growth regime, indicate that crack-growth rates in flattened Nitinol thin-walled tube C(T) samples are essentially unchanged at frequencies between 5 and 50 Hz, although there does appear to be a small but definitive reduction in growth rates at the lower frequency for the lower ΔK levels.

the two frequencies; specifically, da/dN was 3.6×10^{-8} and 3.9×10^{-8} m/cycle at 50 and 5 Hz, respectively, representing a slight 8% increase in growth rate at the lower frequency. Conversely, at $\Delta K = 3 \text{ MPa}\sqrt{\text{m}}$, growth rates were $\sim 21\%$ slower at 5 Hz (7.6×10^{-9} m/cycle), as compared to 50 Hz (9.6×10^{-9} m/cycle).

What these experiments show is that there are essentially no adverse effects of lower frequency on fatigue-crack growth rates in Nitinol over the range from 5 to 50 Hz. If anything, growth rates are marginally slower at 5 Hz, which may be associated with enhanced (oxide-induced) crack closure effects,³¹ or more probably that heat, generated adiabatically due to the *in situ* phase transformation, is more effectively dissipated at the lower frequencies. In terms of design and life prediction analyses, these minimal differences in growth-rate behavior at 5 and 50 Hz do justify the use of higher frequency (~ 50 Hz) fatigue testing to accurately mimic fatigue behavior *in vivo*; moreover, the use of the higher frequency data should not result in nonconservative lifetime predictions.

Effect of thin- versus thick-section material

Although there are only limited fatigue-crack propagation data for superelastic Nitinol in the literature, it is instructive to compare these data with the current results. This is shown in Figure 4, where results in 22–40°C air on thickness-section geometries (thickness $B \sim 9\text{--}10$ mm)^{3,16} are compared with that for thin-strip material ($B \sim 0.2$ mm)¹⁷ and the current results on flattened thin-wall tube material ($B \sim 0.4$ mm), under conditions of $R = 0.1\text{--}0.2$ and frequencies from 10 to 50 Hz. A clear trend of lower fatigue thresholds in the thick-section geometries is apparent. Specifically, the thick-section bar material displays fatigue threshold values of $\Delta K_{\text{th}} \leq 2 \text{ MPa}\sqrt{\text{m}}$, whereas $\Delta K_{\text{th}} \geq 2.5 \text{ MPa}\sqrt{\text{m}}$ for the thin-section strip and flattened tube materials. Interestingly, instability appears to be dependant more upon the testing frequency than the product form; 50-Hz tests in bar and thin-walled tube show an instability at $K_{\text{max}} \sim 10 \text{ MPa}\sqrt{\text{m}}$, as compared to values of $K_{\text{max}} \sim 30 \text{ MPa}\sqrt{\text{m}}$ in thick bar and thin strip tested at 10 and 15 Hz, respectively.

The precise reason for the difference in near-threshold fatigue behavior, which would have the most significant influence on fatigue lifetimes, is not altogether clear. It is interesting to speculate, however, that since McKelvey and Ritchie¹⁶ concluded for their thick-section bar material that the enhanced triaxial (plane-strain) constraint at the growing crack tip could act to suppress the transformation (as it involves a negative dilation), such that crack growth

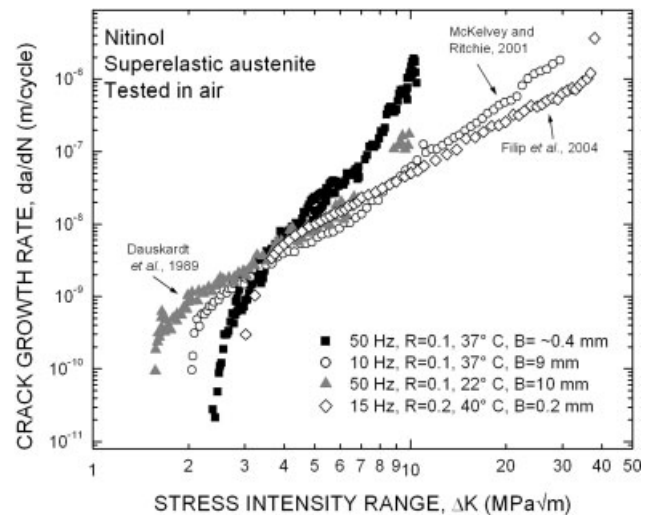


Figure 4. A comparison of published fatigue-crack growth data for superelastic Nitinol with current results. All tests were conducted in air at temperatures between 22 and 40°C at load ratios of 0.1–0.2, with frequencies of 10–50 Hz. Note how the thicker section geometries (thickness $B \sim 9\text{--}10$ mm)^{3,16} display the lowest fatigue thresholds ($\Delta K_{\text{th}} \leq 2 \text{ MPa}\sqrt{\text{m}}$), whereas the thin-section geometries ($B \sim 0.2\text{--}0.4$ mm) have threshold values of $\Delta K_{\text{th}} \geq 2.5 \text{ MPa}\sqrt{\text{m}}$ ¹⁷ (current study). However, instability is dependant upon the testing frequency rather than the product form as evidenced by $K_{\text{max}} \sim 10 \text{ MPa}\sqrt{\text{m}}$ in tests conducted at 50 Hz, when compared to values of $K_{\text{max}} > 30 \text{ MPa}\sqrt{\text{m}}$ in those performed at 10–15 Hz.

in these thick sections may involve crack advance solely into nontransforming austenite. In contrast, *in situ* synchrotron X-ray diffraction studies on the current thin-section tube material (which is not in plane strain) clearly show the formation of stress-induced martensite in the crack-tip region.³⁵ This difference in microstructure into which the crack may be growing is significant for two competing reasons. First, the higher thresholds in the thin-section material may be associated with the fact that resistance to fatigue-crack growth in Nitinol is definitively higher, particularly at near-threshold levels, in the martensitic structure, compared to either stable or superelastic austenite^{3,16} (e.g., Fig. 5).¹⁶ Second, there is a possibility that with increasing ΔK levels the occurrence of the transformation may result in progressively faster growth rates, as shown by the thin-section material. As the transformation involves a small negative dilation, the constraint of the surrounding (nontransformed) material may lead to an additional (positive) contribution to the stress intensity experienced at the crack tip; indeed, Yan et al.⁴ predict that the local stress intensity at the crack tip may be increased by as much as 13%. However, this latter effect will only be relevant where transformation-zone sizes remain small compared to sample dimensions. With the prevalent effects of microstruc-

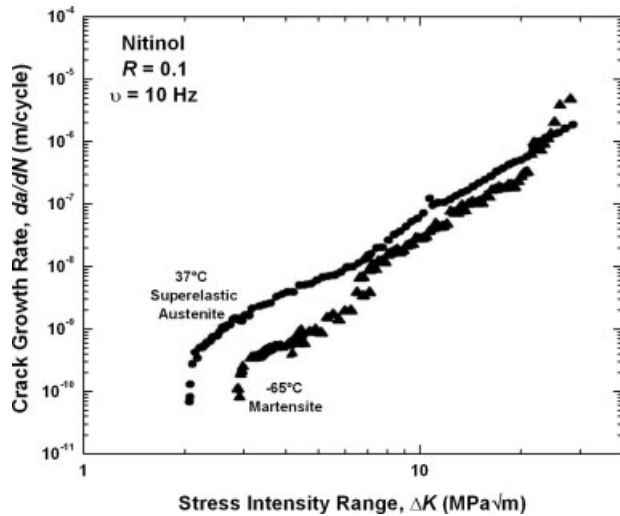


Figure 5. Fatigue-crack growth rates for superelastic and martensitic Nitinol tested using 9-mm thick C(T) samples cut from a rod. Resistance to fatigue-crack growth is clearly enhanced in the martensitic microstructure. Specifically, the fatigue threshold for martensite is roughly 1 MPa $\sqrt{\text{m}}$ higher than that for superelastic austenite (after Ref. 16).

ture on the mechanical properties of Nitinol well documented, it is quite possible that the differences in the microstructure (e.g., inclusion composition and volume percent, texture, and grain size) between the various product forms might offer a simple explanation for the variations in fatigue-crack growth properties.

CONCLUSIONS

A fracture mechanics-based methodology has been employed here to provide the basic engineering parameters (ΔK_{th} , C , m) for assessing the quantitative effect of flaws of the fatigue life of devices manufactured from Nitinol tube. This method offers a compliment to the prevalent total-life ($S-N$) data in the literature by providing a means for calculating critical flaw sizes to be detected during manufacture of devices. Because cracks that are grown in the laboratory experiments may be sharper than actual flaws in the material (e.g., inclusions), lifetime estimates based upon these fracture mechanics parameters offer an invariably conservative estimate.

Based on an experimental study to characterize the fatigue-crack propagation behavior of Nitinol in superelastic austenitic material pertinent to the manufacture of endovascular stents (flattened, $\sim 400\text{-}\mu\text{m}$ thick, thin-walled tube), the following conclusions can be made:

1. Fatigue-crack growth rates, measured over the range from 10^{-11} to 10^{-6} m/cycle in 37°C air in C(T) samples oriented at 45° to the tube drawing direction, show a marked dependence on the (positive) load ratio, which was varied in this study between $R = K_{\text{min}}/K_{\text{max}} = 0.1\text{--}0.7$. Specifically, near-threshold growth rates are increased and ΔK_{th} fatigue thresholds are decreased with increasing R . Compared to most metallic and intermetallic alloys, ΔK_{th} threshold values are low, varying from 2.5 MPa $\sqrt{\text{m}}$ at $R = 0.1$ to 1.4 MPa $\sqrt{\text{m}}$ at $R = 0.7$.
2. Crack-growth rates cannot be scaled solely in terms of ΔK or K_{max} . Accordingly, fatigue-crack growth properties in Nitinol are described in terms of a modified Paris-law relationship: $da/dN = C'(K_{\text{max}})^n(\Delta K)^p$, where the dependence on ΔK is approximately twice as significant as on K_{max} . With respect to the exponents, $p \sim 2.7$ and $n \sim 0.8\text{--}1.0$, consistent with the behavior of most metallic and intermetallic alloys.
3. No significant effect of test frequency between 5 and 50 Hz was seen on fatigue-crack growth rates in both 37°C air and simulated body fluid (HBSS) environments, for tests conducted under constant ΔK conditions (at $R = 0.1$ and 0.5 for air and HBSS, respectively) within the steady-state (Paris) growth-rate regime. This implies that design and life prediction for biomedical devices can be reliably based on high-frequency (~ 30 Hz) fatigue data, without compromising the conservative nature of the analyses.
4. Comparison of the current results with the limited studies in the literature on fatigue-crack growth in superelastic Nitinol in different product forms (i.e., strip and bar) reveals that thin-section Nitinol (with thicknesses of 0.2–0.4 mm) displays quite different near-threshold crack-growth behavior to thick-section material (with thickness of 9–10 mm). Specifically, thin-section Nitinol shows higher fatigue thresholds ($\Delta K_{\text{th}} \geq 2.5$ MPa $\sqrt{\text{m}}$, as compared to values of $\Delta K_{\text{th}} \leq 2$ MPa $\sqrt{\text{m}}$ in thick-section material).

Particular thanks are due to Drs. Tom Duerig and Alan Pelton of NDC for their financial support, supply of Nitinol samples, and for innumerable helpful discussions.

References

1. Wayman CM, Duerig TW. Chapter 1: An introduction to martensite and shape memory. In: Duerig TW, Melton KN, Stöckel D, Wayman CM, editors. *Engineering Aspects of Shape Memory Alloys*. London: Butterworth-Heinemann; 1990. pp 3–20.
2. Holtz RL, Sadananda K, Imam MA. Fatigue thresholds of Ni-Ti alloy near the shape memory transition temperature. *Int J Fatigue* 1999;21:S137–S145.
3. Dauskardt RH, Duerig TW, Ritchie RO. Effects of in situ phase transformation on fatigue-crack propagation in tita-

- nium-nickel shape-memory alloys. In: Otsuka K, Shimizu K, editors. Shape Memory Materials (Proceedings of the MRS International Meeting on Advanced Materials, Vol. 9) Pittsburgh, PA: Materials Research Society; 1989. pp 243–249.
4. Yan W, Wang CH, Zhang XP, Mai YW. Effect of transformation volume contraction on the toughness of superelastic shape memory alloys. *Smart Mater Struct* 2002;11:947–955.
 5. Evans AG, Cannon RM. Toughening of brittle solids by martensitic transformations. *Acta Metall* 1986; 34:761–800.
 6. Dauskardt RH, Marshall DB, Ritchie RO. Cyclic fatigue-crack propagation in Mg-PSZ ceramics. *J Am Ceram Soc* 1990;73: 893–903.
 7. Pederson OM, Aslaksen A, Vik-Mo H. Ultrasound measurement of the luminal diameter of the abdominal aorta and iliac arteries in patients without vascular disease. *J Vasc Surg* 1993;17:596–601.
 8. US Department of Health and Human Services. Guidance for the submission of research and marketing applications for interventional cardiology devices. Washington, DC: US Department of Health and Human Services, US FDA; 1995.
 9. Tabanlı RM, Simha NK, Berg BT. Mean stress effects on fatigue of NiTi. *Mater Sci Eng A* 1999;273–275:644–648.
 10. Tolomeo D, Davidson S, Santinoranont M. Cyclic properties of superelastic Nitinol: Design implications. In: Russell SM, Pelton AR, editors. Proceedings of the International Conference on Shape Memory and Superelastic Technologies. Menlo Park, CA: SMST Society; 2000. pp 471–476.
 11. Wurzel D, Hornbogen E. The influence of thermomechanical treatments on fatigue behavior of NiTi alloys. In: Russell SM, Pelton AR, editors. Proceedings of the International Conference on Shape Memory and Superelastic Technologies. Menlo Park, CA: SMST Society; 2000. pp 383–390.
 12. Eggeler G, Hornbogen E, Yawny A, Heckmann A, Wagner M. Structural and functional fatigue of NiTi shape memory alloys. *Mater Sci Eng A* 2004;378:24–33.
 13. Wagner M, Sawaguchi T, Kasträter G, Höffken D, Eggeler G. Structural fatigue of pseudoelastic NiTi shape memory wires. *Mater Sci Eng A* 2004;378:105–109.
 14. Prymak O, Klocke A, Kahl-Nieke B, Eppel M. Fatigue of orthodontic nickel-titanium (NiTi) wires in different fluids under constant mechanical stress. *Mater Sci Eng A* 2004;378: 110–114.
 15. McKelvey AL, Ritchie RO. Fatigue crack propagation in Nitinol, a shape-memory and superelastic endovascular stent material. *J Biomed Mater Res* 1999;47:301–308.
 16. McKelvey AL, Ritchie RO. Fatigue-crack growth behavior in the superelastic and shape-memory alloy Nitinol. *Metall Mater Trans A* 2001;32:731–743.
 17. Filip P, Paliwal M, Mazanec K. Fatigue behavior of pseudoelastic TiNi thin strips in air and body fluid simulated environments. *Zeitschrift für Metallkunde* 2004;95:356–361.
 18. Robertson SW, Gong XY, Ritchie RO. Effect of product form and heat treatment on the crystallographic texture of austenitic Nitinol. *J Mater Sci* 2006;41:621–630.
 19. American Society of Testing Materials International (Subcommittee E08.06). Standard test method for measurement of fatigue crack growth rates. In: ASTM Book of Standards, Vol. 3.01. West Conshohocken, PA: ASTM; 2005. Standard E 647.
 20. Ritchie RO. Mechanisms of fatigue crack propagation in metals, ceramics and composites: Role of crack-tip shielding. *Mater Sci Eng A* 1988;103:15–28.
 21. Ritchie RO. Mechanisms of fatigue-crack propagation in ductile and brittle solids. *Int J Fract* 1999;100:55–83.
 22. Suresh S, Ritchie RO. Near-threshold fatigue crack propagation: A perspective on the role of crack closure. In: Davidson DL, Suresh S, editors. Fatigue crack growth concepts. Warrendale, PA: TMS-AIME; 1984. pp 227–261.
 23. Suresh S, Zamiski GF, Ritchie RO. Oxide-induced crack closure: An explanation for near-threshold corrosion fatigue crack growth behavior. *Metall Trans A* 1981;12:1435–1443.
 24. Walker N, Beevers CJ. A fatigue crack closure mechanism in titanium. *Fatig Eng Mater Struct* 1979;1:135–148.
 25. Minakawa K, McEvily AJ. On crack closure in the near-threshold region. *Scr Metall* 1981;15:633–636.
 26. Suresh S, Ritchie RO. A geometric model for fatigue crack closure induced by fracture surface roughness. *Metall Trans A* 1982;13:1627–1631.
 27. Shih CF. Relationships between the J-integral and the crack opening displacement for stationary and extending cracks. *J Mech Phys Solids* 1981;29:305–326.
 28. Badrinarayanan K, McKelvey AL, Venkateswara Rao KT, Ritchie RO. Fracture and fatigue-crack growth in ductile-phase toughened molybdenum disilicide: Effects of niobium wire vs. particulate reinforcements. *Metall Mater Trans A* 1996; 27:3781–3792.
 29. Campbell JP, Venkateswara Rao KT, Ritchie RO. On the effect of microstructure on fracture toughness and fatigue-crack growth behavior in γ -based titanium aluminide intermetallics. *Metall Mater Trans A* 1999;30:563–577.
 30. Dauskardt RH, James MR, Porter JR, Ritchie RO. Cyclic fatigue-crack growth in SiC-whisker-reinforced alumina ceramic composite: Long and small-crack behavior. *J Am Ceram Soc* 1992;75:759–771.
 31. Bartlett ML, Hudak SJ Jr. The influence of frequency-dependent crack closure on corrosion fatigue-crack growth. In: Kitagawa H, Tanaka T, editors. Fatigue 90, Vol. 3. Birmingham, UK: Materials and Components Engineering Publications; 1990. pp 1783–1788.
 32. Liu Y, Li Y, Ramesh KT. Rate dependence of deformation mechanisms in a shape memory alloy. *Philos Mag A* 2002;82: 2461–2473.
 33. Nemat-Nasser S, Choi JY, Guo WG, Isaacs JB. Very high strain-rate response of a NiTi shape-memory alloy. *Mech Mater* 2005;37:287–298.
 34. Prince AG, Quarini GL, Morgan JE, Finlay J. Thermomechanical response of 50.7 at.-%Ni–Ti alloy in the pseudoelastic regime. *Mater Sci Technol* 2003;19:561–565.
 35. Robertson SW, Ritchie RO, Mehta A, Gong XY, Pelton A. Ultrahigh resolution *in situ* diffraction characterization of the local mechanics at a growing crack tip in Nitinol. In: Proceedings of the International Conference on Shape Memory and Superelastic Technologies. Menlo Park, CA: SMST Society. Forthcoming.